Dentomaxillofacial Radiology (2022) 51, 20210337

birpublications.org/dmfr

RESEARCH ARTICLE

Multifrequency magnetic resonance elastography-based tomoelastography of the parotid glands–feasibility and reference values

[1]Fabian Henry Jürgen Elsholtz, [1,2]Rolf Reiter, [3]Stephan Rodrigo Marticorena Garcia, [4]Jürgen Braun, [3]Ingolf Sack, [1]Bernd Hamm and [1]Lars-Arne Schaafs

[1]Department of Radiology, Charité – Universitätsmedizin Berlin, corporate member of Freie Universität Berlin and Humboldt-Universität zu Berlin, Campus Benjamin Franklin, Berlin, Germany; [2]Berlin Institute of Health at Charité – Universitätsmedizin Berlin, Berlin, Germany; [3]Department of Radiology, Charité – Universitätsmedizin Berlin, corporate member of Freie Universität Berlin and Humboldt-Universität zu Berlin, Campus Charité Mitte, Berlin, Germany; [4]Universitätsmedizin Berlin, corporate member of Freie Universität Berlin and Humboldt-Universität zu Berlin, Institute of Medical Informatics, Campus Charité Mitte, Berlin, Germany

Objectives: Accurate radiological differentiation of parotid tumors remains challenging despite recent technical advances in quantitative medical imaging. Multifrequency magnetic resonance elastography (MRE) could provide additional information on viscoelastic properties of normal and abnormal biological tissues. This study investigates the feasibility of MRE of the parotid glands in healthy participants and provides first reference values.
Methods: 20 healthy participants underwent multifrequency MRE of both parotid glands at 3 Tesla. Shear waves at frequencies of 25, 30, 40, and 50 Hz were introduced into the participants' heads through the occiput using pressurized-air actuators. Shear wave speed (SWS) and loss angle of the shear modulus (ϕ) were reconstructed by tomoelastography post-processing as surrogate parameters for tissue stiffness and viscosity or fluidity. 10 participants underwent repeated MRE to determine test–retest reliability based on intraclass correlation coefficients.
Results: All MRE datasets acquired could be included in the analysis. Mean SWS was 0.97 ± 0.13 m/s, and mean ϕ was 0.59 ± 0.05 rad, each for both sides combined and without notable lateral difference (p = 0.88/0.87). Test–retest reliability was good for SWS (ICC = 0.84 for both sides/ICC = 0.77 for the right side/ICC = 0.79 for the left side) and good to excellent for ϕ(ICC = 0.94/0.86/0.90).
Conclusions: Multifrequency MRE of the parotid glands is feasible and reliable. This technique, therefore, is a promising method for investigating the viscoelastic properties of salivary gland tumors in future studies.
Dentomaxillofacial Radiology (2022) **51**, 20210337. doi: 10.1259/dmfr.20210337

Cite this article as: Elsholtz FHJ, Reiter R, Marticorena Garcia SR, Braun J, Sack I, Hamm B, et al. Multifrequency magnetic resonance elastography-based tomoelastography of the parotid glands–feasibility and reference values. *Dentomaxillofac Radiol* 2022; **51**: 20210337.

Keywords: Magnetic resonance elastography; Tomoelastography; Viscoelasticity; Head and neck; Parotid glands

Correspondence to: Dr. med. Fabian Henry Jürgen Elsholtz, E-mail: fabian.elsholtz@charite.de

Received 21 July 2021; revised 24 August 2021; accepted 07 September 2021

Introduction

Tumors of the major salivary glands (parotid, submandibular, and sublingual glands) account for about 3% of all tumors in the human body.[1] Both the likelihood of tumor occurrence and the presence of a benign entity are positively correlated with salivary gland size. Thus, most tumors of the major salivary glands are localized in the parotid gland, where benign entities like pleomorphic adenoma predominate.[2,3] For radiologists, the differential diagnoses of these tumors and a certain overlap in their imaging appearance pose a challenge in clinical routine. However, differentiation between benign and malignant entities is essential, as the suspicion of malignancy may trigger the indication for superficial or lateral parotidectomy and also the need for dedicated cervical lymph node staging.[1] With its high soft tissue contrast, MRI has become the imaging modality of choice when a parotid tumor is suspected. Multiparametric (MP-)MRI using (semi-)quantitative techniques such as dynamic contrast-enhanced MRI (DCE-MRI) or diffusion-weighted imaging (DWI) has been evaluated for its additional value, and a combination of these techniques has been shown to provide features that are suggestive of a specific entity.[4–7] However, evaluation of these imaging features is not possible without contrast medium administration. Magnetic resonance elastography (MRE) is a quantitative imaging technique where externally generated acoustic waves are coupled into the body to provide viscoelastic parameter maps of the tissue examined. Surrogate parameters for tissue stiffness and fluidity can be computed by tomoelastography processing and diagrammed as high-resolution maps. MRE has already been successfully used to assess tumors in other organs such as the brain, the liver, or the prostate.[8–10] Most recently, a first successful application of MRE in the head and neck (HN) region has been described.[11] Therefore, MRE appears to be a promising addition to existing MRI techniques that can contribute to the differentiation of normal and abnormal tissues in the HN region using contrast based on mechanical properties. The aim of this study was to evaluate multifrequency MRE of the parotid glands and to provide reference values of organ-specific tissue stiffness in a group of healthy participants as a basis for further studies to characterize parotid gland tumors in patients.

Methods and materials

Study design and patient selection

This prospective study was approved by the institutional review board (EA1/066/19), and written informed consent of all participants was obtained. Pre-existing conditions involving the major salivary glands (*e.g.* known tumors, prior surgery), contraindications to MRI (*e.g.* implanted non-MRI-compatible medical devices or magnetic foreign bodies) as well as pregnancy were defined as exclusion criteria. Orthodontic retainers and teeth implants were deliberately not defined as exclusion criteria.

20 participants (6 female, 14 male) with a mean age of 32 years (range 28–38 years) were included in this study.

Three of the participants examined had fixed orthodontic retainers consisting of a wire and composite on the lingual and palatal surface of the upper and lower front teeth (11–13, 21–23, 31–33, 41–43), and one participant had an implant for tooth 27.

MRE setup and examination protocol

Participants were examined in a 3-Tesla scanner (Magnetom Skyra, Siemens Healthineers, Erlangen, Germany) with a combined head/neck coil. First, axial fat-saturated T_2 weighted images and axial T_1 weighted images were acquired for anatomical evaluation of the parotid glands. Second, MRE was conducted. Shear waves were introduced into the parotid glands by two pressurized-air drivers identical to those detailed elsewhere.[11] The two drivers were mounted under a slightly concavely curved plate serving as occipital contact surface as shown in Figure 1. Mechanical vibration frequencies were 25, 30, 40, and 50 Hz, which were

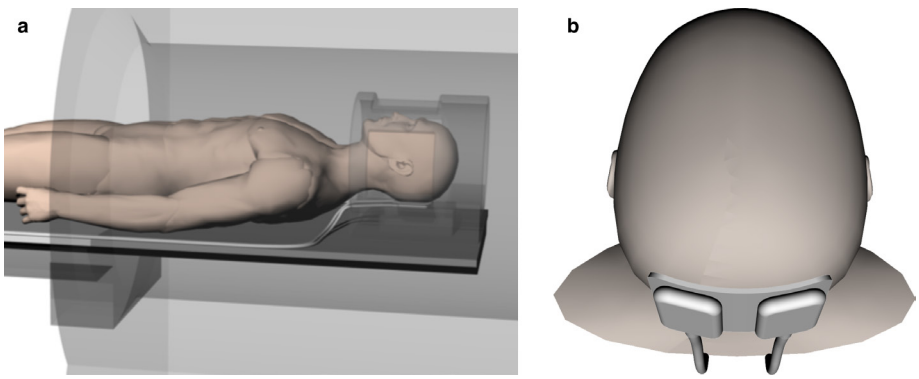

Figure 1 (a, b) Schematic drawing of the MRE setup. The participants' head was positioned in a combined head/neck coil (a) and pressurized-air drivers mounted under a curved plate were used to couple mechanical vibrations into the occiput (b). MRE, magnetic resonance elastography.

consecutively acquired with three wave field components over 8 wave dynamics in 48 imaging slices of primary axial orientation and 2 mm slice thickness without a slice gap using a single-shot spin-echo echoplanar imaging MRE sequence.[12] The following imaging parameters were used: matrix size = 128 x 128 cm, field of view (FOV) = 1280 x 1280 cm^2, repetition time (TR) = 3280 ms, time to echo (TE) = 69 ms, and total scan time = 5:30 min.

MRE data processing

Tomoelastography data processing was applied to the complex-valued multifrequency MRE datasets. Wave-number-based multifrequency dual elastovisco (k-MDEV) inversion was used for the reconstruction of shear wave speed (SWS) (in m/s) maps to serve as a surrogate parameter of tissue stiffness. Laplacian-based MDEV inversion was used for reconstruction of the loss angle of the shear modulus (φ in rad) as a surrogate parameter of tissue viscosity or fluidity (ranging from 0 – purely solid properties to 2π – purely fluid properties). Both the *k*-MDEV and MDEV processing pipeline can be publicly accessed via https://bioqic-apps.charite.de.

MRE image analysis

Two radiologists subspecialized in HN imaging (6 and 7 years of experience) analyzed MRE data sets. First, the primary wave images were assessed for the presence of waves propagating through the tissues originating from the occipital coupling. Second, SWS and ϕ maps were analyzed after importing them into the PACS viewer Visage Client v. 7.1.15 (Visage Imaging GmbH, Berlin, Germany). This was accomplished by identifying the parotid glands in the axially oriented magnitude map and drawing polygonal two-dimensional regions of interest (ROIs) along their borders, avoiding obvious artifacts. Those ROIs were then automatically transferred to the SWS and φ maps. The values measured in each participant were averaged for both sides taken together and each side separately. An example of MRE dataset analysis is presented in Figure 2.

Statistical analysis

Statistical analysis of all MRE data was performed using R (via RStudio v. 1.3.1093, PBC, Boston, MA) and its "plotrix" and "irr" packages. All SWS and ϕ data acquired by ROI measurement were interpreted for both sides taken together and for the right and left side separately. Data from all 20 participants were tested for normal distribution using the Shapiro–Wilk test, and mean, range, median, standard deviation, standard error of the mean, and 95% confidence interval were computed. Both parameters were tested for significant differences in means between sides of the parotid gland by applying a paired *t*-test, and statistical significance was assumed for p values < 0.05. Absolute differences in means, ranges of absolute differences in means, and intraclass correlation coefficient (ICC) were calculated for SWS and ϕ data of all 10 participants who underwent repeat examination.[13] ICC values were interpreted as suggested by Koo and Li[14]:

- < 0.5: "poor"
- 0.5–0.75: "moderate"
- 0.75–0.9: "good"
- 0.9–1: "excellent"

Additionally, separate Bland–Altman plots for SWS and φ were created using the "BlandAltmanLeh" package (Figure 3).

Results

Sufficient wave propagation was observed in all 30 wave imaging data sets acquired in the study participants and all datasets could be included in the analysis. The Shapiro–Wilk test revealed a normal distribution of SWS and ϕ data for both sides taken together and for the right and left side separately.

Mean SWS was 0.97 ± 0.13 m/s for both sides combined without a notable lateral difference (right side: 0.97 ± 0.13 m/s, left side: 0.97 ± 0.13 m/s, p = 0.88). Similarly, no laterality was seen in φ with a mean of 0.59

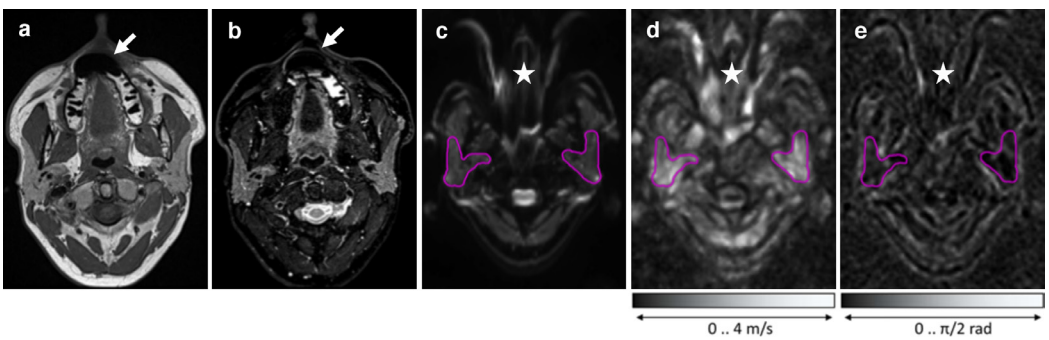

Figure 2 (a–e) Example case of a 30-year-old male participant showing acquired axial anatomic T_1 weighted (a) and T_2 weighted (b) images as well as MRE dataset analysis using polygonal ROIs drawn around the borders in three consecutive slices of the axial MRE-magnitude map (c) and then transferred to the SWS map (d) and φ map (e). Despite artifacts (white stars) resulting from orthodontic retainers (indicated by white arrows and stars), the parotid glands were adequately depicted in the parameter maps. MRE, magnetic resonance elastography; ROI, region of interest; SWS, shear wave speed.

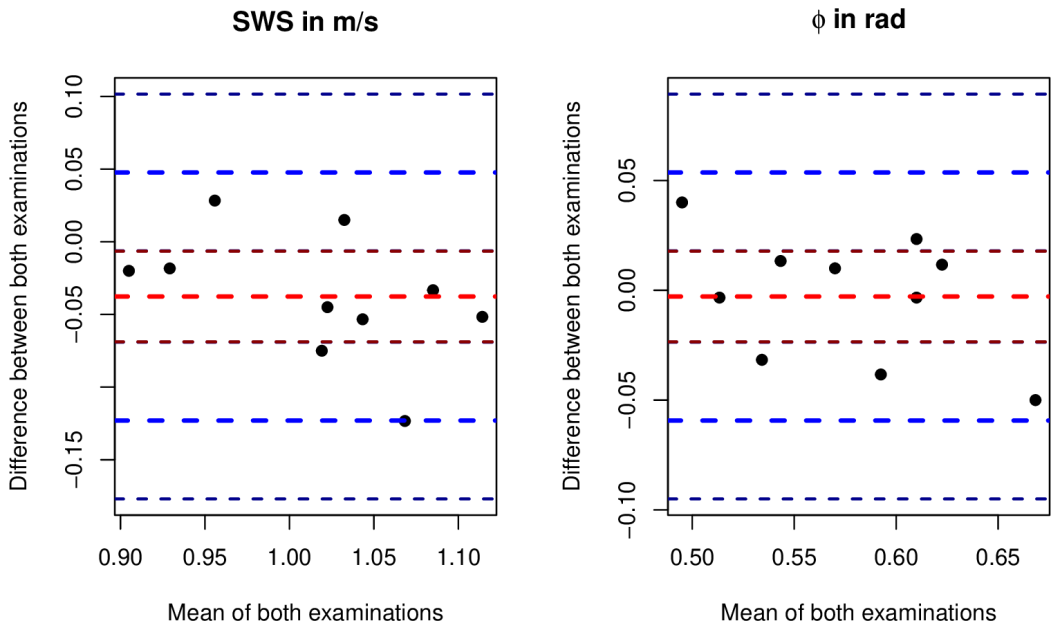

Figure 3 Bland–Altman plots of agreement between both examinations for SWS and φ. Single red bold dashed line = mean difference; paired blue bold dashed lines = 95% limits of agreement (paired dark thin red and blue dashed lines = lower and upper bounds of 95% confidence interval).

± 0.05 rad for both sides combined (right side: 0.59 ± 0.06 rad, left side: 0.58 ± 0.06, p = 0.87). All results of the first examination of all 20 participants are summarized in Table 1.

Test–retest reliability determined by performing a second examination in ten participants was good for SWS (ICC = 0.84 for both sides/ICC = 0.77 for the right side/ICC = 0.79 for the left side) and good to excellent for ϕ (ICC = 0.94/ICC=0.86/ICC=0.90). Mean absolute differences in mean SWS and mean ϕ between the first and second examinations were 0.05 m/s for both sides combined, 0.05 m/s for the right side, and 0.05 m/s for the left side, and 0.02 rad, 0.04 rad, and 0.05 rad, respectively. All results regarding test–retest reliability are summarized in Table 2. Bland–Altman plots presented in Figure 3 show the agreement between both examinations.

Discussion

To the best of our knowledge, this is the first study reporting tissue stiffness and fluidity estimates for the parotid glands obtained by using multifrequency MRE.

Our study found an average SWS of 0.97 m/s and an average ϕ of 0.59 rad for parotid gland tissue.

The same MRE setup has already been used in a patient with mandibular ameloblastoma and published as a case report.[11] In this case, MRE revealed not only abnormal stiffness and fluidity of the primary tumor compared with the healthy opposite side but also abnormal stiffness of a local level Ib lymph node smaller than 1 cm, which was later confirmed to be metastatic by histopathology. This first case report suggests that MRE has the potential to even detect smaller tumors in the parotid gland provided they differ in stiffness and

Table 1 Findings for MRE surrogate parameters of tissue stiffness (SWS) and fluidity (ϕ) in the initial examination of all 20 participants

	SWS (mls)			*ϕ (rad)*		
	Both	***Right***	***Left***	***Both***	***Right***	***Left***
Mean	0.97	0.97	0.98	0.59	0.59	0.58
Range	0.72–1.19	0.73–1.21	0.72–1.20	0.51–0.69	0.47–0.69	0.46–0.69
Median	0.98	0.97	1.00	0.59	0.59	0.58
SD	0.13	0.13	0.13	0.05	0.06	0.06
SEM	0.03	0.03	0.03	0.01	0.01	0.01
CI	0.92–1.03	0.91–1.03	0.92–1.04	0.56–0.61	0.56–0.62	0.56–0.61

MRE, magnetic resonance elastography; SD, Standard deviation; SEM, Standard error of the mean;SWS, shear wave speed.
95% confidence interval (lower bound - upper bound).

Table 2 Results for test–retest reliability in 10 participants examined twice

	SWS (mls)			*ϕ (rad)*		
	Both	***Right***	***Left***	***Both***	***Right***	***Left***
Δabsolute	0.05	0.05	0.05	0.02	0.04	0.05
Range	0.02–0.12	0.01–0.14	0.01–0.18	0.01–0.05	0.01–0.07	0.02–0.08
ICC	0.84	0.77	0.79	0.94	0.86	0.80

ICC, Intraclass correlation coefficient; SWS, shear wave speed; $\Delta_{absolute}$, Mean absolute differences in mean parameter values between both examinations.

fluidity from the reference values obtained in this pilot study.

While we here report the first application of MRE in the major salivary glands, ultrasound shear wave elastography of these organs has been addressed in several studies before. Most frequently, as in the study of Bhatia et al, overlaps were observed between different benign as well as benign and malignant entities, which at least limits the clinical usefulness of the method.[15] However, studies investigating applications of the technique for assessing diffuse parenchymal changes of the major salivary glands have also been reported. A recently published study by Arslan et al[16] concludes ultrasound SWE to be an effective technique for predicting interstitial fibrosis and the degree of histological damage in patients with primary Sjögren's syndrome.

In a previously published study investigating the MRE of abdominal organs in healthy subjects, pancreatic tissue stiffness values of 1.20 ± 0.12 m/s were found.[17] Thus, together with our results, we can assume a similar tissue stiffness of the pancreas and parotid gland (0.97 ± 0.13 m/s). This is not surprising given that the parotid and the exocrine portion of the pancreas are purely serous glands and thus have similar histologic structures.[18] On the other hand, the robustness of the fluidity surrogate parameter, ϕ, observed in our study may be of particular importance in the diagnostic evaluation of parotid gland tumors using MRE in future studies. Previous publications have already underlined the importance of the higher fluidity of tumors for their ability to infiltrate surrounding tissue.[10,19]

The combination of different morphological and functional MRI techniques to improve the differentiation of tumor entities affecting the parotid gland has been postulated by several investigators.[4,20,21] In this sense, MRE could contribute a useful quantitative component for tumor characterization, and could furthermore be useful in diffuse parenchymal disease.

The uncompromised evaluability of images from participants with metallic orthodontic retainers (Figure 2) and dental implants was particularly encouraging as such materials are likely to be encountered in presumably older patient populations that should be investigated in future clinical studies.

While test–retest reliability was good for SWS, it was good to even excellent for ϕ. Three factors should be considered concerning reproducibility. First, the well-known sensitivity of EPI sequences to susceptibilities – which is a severe problem especially in the HN region – might cause artifacts depending on how participants are positioned for the examination.[22,23] Second, physiological differences such as between pre- and post-prandial states or different levels of hydration could play a role. Such effects have already been reported for the liver, the spleen, the pancreas, and the kidneys.[17] Third, the small number of participants must be considered independently of possible influences as just outlined. In addition to expected inter- individual variability, the size and constitution of intraparotid lymph nodes and vessels may have had an excessive effect on our statistical results due to the relatively small number of participants.

This study has some limitations. First, only a small sample of participants was studied, but this is acceptable as we performed a hypothesis-generating study. Second, the altogether young study participants were highly compliant during the MRE examination. How the feasibility and evaluability of parotid MRE will be affected when actual patients, who are likely to be older and presumably more morbid, are examined remains to be seen.

Conclusion

Multifrequency MRE of the parotid glands is feasible and reliable. This technique, therefore, is a promising candidate for investigating the viscoelastic properties of salivary gland tumors in future studies.

Competing interests

Fabian Henry Jürgen Elsholtz: None declared. Rolf Reiter: None declared. Stephan Rodrigo Marticorena Garcia: None declared. Jürgen Braun: None declared. Ingolf Sack: None declared. Bernd Hamm: Reports grant from Abbott, Actelion Pharmaceuticals, Bayer Schering Pharma, Bayer Vital, BRACCO Group, Bristol-Myers Squibb, Charité Research Organisation GmbH, Deutsche Krebshilfe, Dt. Stiftung für Herzforschung, Essex Pharma, European Society of Radiology, Fibrex Medical Inc., Focused Ultrasound Surgery Foundation, Fraunhofer Gesellschaft, Guerbet, INC Research, InSightec Ltd., IPSEN Pharma, Kendle/MorphoSys AG, Lilly GmbH, Lundbeck GmbH, MeVis Medical Solutions AG, Nexus Oncology, Novartis, Parexel CRO

Service, Perceptive, Pfizer GmbH, Philipps, sanofi-aventis S.A., Siemens, Spectranetics GmbH, Terumo Medical Corporation, TNS Healtcare GmbH, Toshiba, UCB Pharma, Wyneth Pharma, Zukunftsfonds Berlin (TSB). Lars-Arne Schaafs: None declared.

Funding

Fabian Henry Jürgen Elsholtz is partially funded by the Deutsche Forschungsgemeinschaft (DFG, German Research Foundation) – project number 372486779 - SFB 1340. Rolf Reiter is participant in the BIH – Charité Digital Clinician Scientist Program funded by the Charité – Universitätsmedizin Berlin, the Berlin Institute of Health, and the Deutsche Forschungsgemeinschaft (DFG, German Research Foundation). Stephan Rodrigo Marticorena Garcia received funding from the Deutsche Forschungsgemeinschaft (DFG, German Research Foundation) – project number 467843609. Open Access funding enabled and organized by Projekt DEAL.

REFERENCES

1. Thoeny HC. Imaging of salivary gland tumours. *Cancer Imaging* 2007; **7**: 52–62. doi: https://doi.org/10.1102/1470-7330.2007.0008
2. Abdel Razek AAK, Mukherji SK. State-Of-The-Art imaging of salivary gland tumors. *Neuroimaging Clin N Am* 2018; **28**: 303–17. doi: https://doi.org/10.1016/j.nic.2018.01.009
3. Maraghelli D, Pietragalla M, Cordopatri C, Nardi C, Peired AJ, Maggiore G, et al. Magnetic resonance imaging of salivary gland tumours: key findings for imaging characterisation. *Eur J Radiol* 2021; **139**: 109716. doi: https://doi.org/10.1016/j.ejrad.2021.109716
4. Habermann CR, Arndt C, Graessner J, Diestel L, Petersen KU, Reitmeier F, et al. Diffusion-weighted echo-planar MR imaging of primary parotid gland tumors: is a prediction of different histologic subtypes possible? *AJNR Am J Neuroradiol* 2009; **30**: 591–6. doi: https://doi.org/10.3174/ajnr.A1412
5. Thoeny HC, De Keyzer F, King AD. Diffusion-Weighted MR imaging in the head and neck. *Radiology* 2012; **263**: 19–32. doi: https://doi.org/10.1148/radiol.11101821
6. Lam PD, Kuribayashi A, Imaizumi A, Sakamoto J, Sumi Y, Yoshino N, et al. Differentiating benign and malignant salivary gland tumours: diagnostic criteria and the accuracy of dynamic contrast-enhanced MRI with high temporal resolution. *Br J Radiol* 2015; **88**: 20140685. doi: https://doi.org/10.1259/bjr.20140685
7. Coudert H, Mirafzal S, Dissard A, Boyer L, Montoriol P-F. Multiparametric magnetic resonance imaging of parotid tumors: a systematic review. *Diagn Interv Imaging* 2021; **102**: 121–30. doi: https://doi.org/10.1016/j.diii.2020.08.002
8. Thompson SM, Wang J, Chandan VS, Glaser KJ, Roberts LR, Ehman RL, et al. Mr elastography of hepatocellular carcinoma: correlation of tumor stiffness with histopathology features-Preliminary findings. *Magn Reson Imaging* 2017; **37**: 41–5. doi: https://doi.org/10.1016/j.mri.2016.11.005
9. Reiss-Zimmermann M, Streitberger K-J, Sack I, Braun J, Arlt F, Fritzsch D, et al. High resolution imaging of viscoelastic properties of intracranial tumours by Multi-frequency magnetic resonance elastography. *Clin Neuroradiol* 2015; **25**: 371–8. doi: https://doi.org/10.1007/s00062-014-0311-9
10. Asbach P, Ro S-R, Aldoj N, Snellings J, Reiter R, Lenk J, et al. In vivo quantification of water diffusion, stiffness, and tissue fluidity in benign prostatic hyperplasia and prostate cancer. *Invest Radiol* 2020; **55**: 524–30. doi: https://doi.org/10.1097/RLI.0000000000000685
11. Beier M, Sack I, Beck-Broichsitter B, Hamm B, Marticorena Garcia SR. Tomoelastography for non-invasive detection of ameloblastoma and metastatic neck lymph nodes. *BMJ Case Rep* 2020; **13**: e23593009 Sep 2020. doi: https://doi.org/10.1136/bcr-2020-235930
12. Tzschätzsch H, Guo J, Dittmann F, Hirsch S, Barnhill E, Jöhrens K, et al. Tomoelastography by multifrequency wave number recovery from time-harmonic propagating shear waves. *Med Image Anal* 2016; **30**: 1–10. doi: https://doi.org/10.1016/j.media.2016.01.001
13. Shrout PE, Fleiss JL. Intraclass correlations: uses in assessing rater reliability. *Psychol Bull* 1979; **86**: 420–8. doi: https://doi.org/10.1037/0033-2909.86.2.420
14. Koo TK, Li MY. A guideline of selecting and reporting intraclass correlation coefficients for reliability research. *J Chiropr Med* 2016; **15**: 155–63. doi: https://doi.org/10.1016/j.jcm.2016.02.012
15. Bhatia KSS, Cho CCM, Tong CSL, Lee YYP, Yuen EHY, Ahuja AT. Shear wave elastography of focal salivary gland lesions: preliminary experience in a routine head and neck us clinic. *Eur Radiol* 2012; **22**: 957–65. doi: https://doi.org/10.1007/s00330-011-2364-3
16. Arslan S, Durmaz MS, Erdogan H, Esmen SE, Turgut B, Iyisoy MS. Two-dimensional shear wave elastography in the assessment of salivary gland involvement in primary Sjögren's syndrome. *J Ultrasound Med* 2020; **39**: 949–56. doi: https://doi.org/10.1002/jum.15179
17. Dittmann F, Tzschätzsch H, Hirsch S, Barnhill E, Braun J, Sack I, et al. Tomoelastography of the abdomen: tissue mechanical properties of the liver, spleen, kidney, and pancreas from single MR elastography scans at different hydration states. *Magn Reson Med* 2017; **78**: 976–83. doi: https://doi.org/10.1002/mrm.26484
18. Rakonczay Z, Vág J, Földes A, Nagy K, Nagy Ákos, Hegyi P, et al. Chronic inflammation in the pancreas and salivary glands--lessons from similarities and differences in pathophysiology and treatment modalities. *Curr Pharm Des* 2014; **20**: 1104–20. doi: https://doi.org/10.2174/13816128113199990415
19. Streitberger K-J, Lilaj L, Schrank F, Braun J, Hoffmann K-T, Reiss-Zimmermann M, et al. How tissue fluidity influences brain tumor progression. *Proc Natl Acad Sci U S A* 2020; **117**: 128–34. doi: https://doi.org/10.1073/pnas.1913511116
20. Zheng N, Li R, Liu W, Shao S, Jiang S. The diagnostic value of combining conventional, diffusion-weighted imaging and dynamic contrast-enhanced MRI for salivary gland tumors. *Br J Radiol* 2018; **91**: 20170707. doi: https://doi.org/10.1259/bjr.20170707
21. Wu Q, Zhu L-N, Jiang J-S, Bu S-S, Xu X-Q, Wu F-Y. Characterization of parotid gland tumors using T2 mapping imaging: initial findings. *Acta Radiol* 2020; **61**: 629–35. doi: https://doi.org/10.1177/0284185119875646
22. Jiang J-S, Zhu L-N, Wu Q, Sun Y, Liu W, Xu X-Q, et al. Feasibility study of using simultaneous multi-slice resolve diffusion weighted imaging to assess parotid gland tumors: comparison with conventional resolve diffusion weighted imaging. *BMC Med Imaging* 2020; **20**: 93. doi: https://doi.org/10.1186/s12880-020-00492-1
23. Porter DA, Heidemann RM. High resolution diffusion-weighted imaging using readout-segmented echo-planar imaging, parallel imaging and a two-dimensional navigator-based reacquisition. *Magn Reson Med* 2009; **62**: 468–75. doi: https://doi.org/10.1002/mrm.22024